Vortex dynamics at subcritical currents at microwave frequencies in DyBa2Cu3O7-δ thin films

Banerjee, Tamalika; Bagwe, V.C.; John, J.; Pai, S.P.; Kanjilal, D.

Published in:
Physical Review B

DOI:
10.1103/PhysRevB.69.104533

Publication date:
2004

Vortex dynamics at subcritical currents at microwave frequencies in $DyBa_2Cu_3O_{7-\delta}$ thin films

Tamalika Banerjee, V. C. Bagwe, J. John, S. P. Pai, and R. Pinto
Department of Condensed Matter Physics and Materials Science, Tata Institute of Fundamental Research, Homi Bhabha Road, Mumbai 400 005, India

D. Kanjilal
Nuclear Science Centre, Aruna Asaf Ali Marg, New Delhi 110 067, India

(Received 25 March 2003; revised manuscript received 25 July 2003; published 30 March 2004)

We have investigated the dynamics of vortices at subcritical microwave currents in dc magnetic fields (up to 0.8 T) in epitaxial $DyBa_2Cu_3O_{7-\delta}$ (DBCO) thin films. Microwave measurements were performed using microstrip resonators as test vehicles at 4.88 GHz and 9.55 GHz on laser ablated DBCO thin films in the thickness range 1800–3800 Å. Experimental evidence indicates that the peak effect (PE) observed in surface resistance vs temperature (R_s vs T) plots in applied dc magnetic fields up to 0.8 T is primarily due to the extended defects in thinner films (1800 Å) such as twin boundaries at the substrate($LaAlO_3$)-film interface; whereas, the high density of point defect disorder in thicker ($\geqslant$3000 Å) films is responsible for low R_s and high depinning frequency ω_p. This has been confirmed by generation of columnar defects using 200 MeV Ag ion irradiation which showed that even thicker DBCO films show PE in R_s after the introduction of columnar defects. Further, DBCO films grown on low-twinned $LaAlO_3$ substrates (which cause low density of substrate-related extended defects in the film) have shown PE only at 9.55 GHz but not at 4.88 GHz. Values of ω_p have been calculated from experimental R_s data. ω_p vs T plots obtained for the thinner films show a peak which is a result of the peaks in R_s vs T plots of these films at 4.88 GHz and 9.55 GHz.

DOI: 10.1103/PhysRevB.69.104533 PACS number(s): 74.78.Bz, 61.80.Jh, 85.25.−j

I. INTRODUCTION

The vortex lattice response to ac fields has been widely used to investigate the vortex dynamics of mixed state of type-II superconductors.[1–3] Pinning by material disorder plays a vital role in determining the static as well as the dynamic behavior of vortices.[4–7] Experiments such as magnetic susceptibility, surface impedance,[8,9] and vibrating reed[10,11] have a common feature that a small ac field interacts with the vortices that have penetrated the samples. Towards this end ac susceptibility measurements[12–14] have been extensively used to understand the dynamics of the vortex lattice. In ac susceptibility measurements the variation of critical current density J_c is probed, where the force on the vortices becomes equal to the maximum pinning force. These measurements are typically carried out with an ac excitation field in the range of a few tens of Hz to few MHz.[2] On the other hand, a small microwave excitation (linear regime) induces a current, which is much smaller than the critical current. Hence, with small microwave currents the vortices oscillate about the minimum of the pinning potential and experience a restoring force close to the potential minimum. Hence, the dynamics of vortices is determined by the balance between the pinning and the viscous force.

The competition between intervortex interactions and pinning by defects in weakly pinned type-II superconductors results in an interesting and long studied phenomenon known as ''peak effect'' (PE) in critical currents.[15] The earliest understanding of the phenomenon of PE in driven flux line lattices (FLL), the collective pinning theory,[16] involves the softening of the elastic moduli of the FLL, so that the vortices may settle more deeply into the pinning potential and thus become more difficult to depin. No PE has been observed in thin films which are heavily pinned due to the high density of point defects in them, and until recently peak effect has not been reported at microwave frequencies. While investigating the dynamics of FLL at microwave frequencies at subcritical currents under dc magnetic fields, we have observed PE in surface resistance R_s in pristine and heavy-ion irradiated $DyBa_2Cu_3O_{7-\delta}$ (DBCO) and $YBa_2Cu_3O_{7-\delta}$ (YBCO) thin films.[3,7] Motivated by these observations, we have carried out investigations of the defect structures responsible for the peak effect at microwave frequencies at subcritical currents and calculated depinning frequency ω_p (also termed as pinning frequency by some authors earlier) as a function of temperature from the experimental R_s data for various DBCO film thicknesses. Experimental evidence obtained on twins at the substrate-film interface and with columnar defects generated by swift Ag ion irradiation indicates that the occurrence of a peak in R_s of DBCO films is associated with extended defects; whereas thicker films (pristine) with a high density of point defects as compared to the substrate-related twins have low R_s and a large value of ω_p and they do not show a peak in R_s.

II. EXPERIMENTAL

DBCO films were grown by pulsed laser deposition (PLD) on single crystal $\langle 100 \rangle$ $LaAlO_3$ (LAO) substrates. The optimized growth parameters are 250 mTorr oxygen pressure, 4.5 cm target-substrate distance, and 780 °C substrate temperature. X-ray-diffraction studies showed all films to be epitaxial and *c*-axis oriented normal to the substrate plane. Superconducting transition temperature determined using ac susceptibility and four-probe resistivity measurements was found to be 91 ± 0.2 K. Microwave transmission

measurements were performed on capacitively coupled microstrip resonators having 9 mm length and 175 mm width patterned on $10\times10\times0.5$ mm^3 LAO substrates using UV lithography. DBCO film thickness was varied from 1800 Å to 3800 Å. A Hewlett Packard scalar network analyzer and a synthesized sweeper source were used for the measurements. dc magnetic field varying from 0 to 0.8 T was applied perpendicular to the film plane ($H\|c$) using a conventional electromagnet. Temperature instability during the microwave measurements carried out in a closed cycle He cryocooler was <30 mK. All data presented here are for the zero-field cooled cases. Details of microwave measurements and determination of R_s have been described earlier.[17] Ag ion irradiation was carried out at the 15 UD Pelletron accelerator at Nuclear Science Center, New Delhi using 200 MeV $^{109}Ag^{+14}$ ions at a fluence of 4×10^{10} ions cm^{-2} (corresponding to the matching field, $B_\phi\sim0.8$ T); columnar defects (CD) are created in the DBCO films with this choice of ions and ion energy.

III. RESULTS

Zero-field cooled R_s vs T plots of 2400 Å thick DBCO film at 4.88 GHz (fundamental excitation of the microstrip resonator) for various field values (0–0.8 T) are shown in Fig. 1(a). Figure 1(b) shows similar plots obtained for the same film at 9.55 GHz (first harmonic excitation) at various field values. Evolution of the peak with increasing field can be clearly seen in both the figures although the peaks are less pronounced at 4.88 GHz than at 9.55 GHz. Zero-field cooled R_s vs T plots of 3800 Å thick DBCO film for various field values at 4.88 GHz are shown in Fig. 2(a). Similar plots obtained for the same film at 9.55 GHz at various field values are shown in Fig. 2(b).

The dependence of R_s on film thickness is shown in Figs. 3 and 4. Figure 3(a) shows the zero field R_s vs T plots of DBCO films of thickness varying from 1800 Å to 3800 Å obtained at 4.88 GHz; shown in Fig. 3(b) are the similar plots of these films obtained at 9.55 GHz. The corresponding zero-field cooled plots at the highest field of 0.8 T are shown in Figs. 4(a) and 4(b) for the two resonant frequencies 4.88 GHz and 9.55 GHz, respectively. Peaks in R_s vs T plots are clearly seen at 0.8 T in the two thinner films (1800 Å and 2400 Å) although there is a faint signature of the peak in the thicker films. Measurements were also carried out on one of the thinner films (1800 Å) with field perpendicular to the c axis to find the orientation dependence. The inset in Fig. 4(b) shows the comparison of the R_s vs T plots of 1800 Å film obtained at 0.8 T, 9.55 GHz with field parallel and perpendicular to the c axis. The peak is seen to be much less prominent when the field is applied perpendicular to the c axis.

The measurements carried out after the 200 MeV Ag ion irradiation (at 4×10^{10} ions cm^{-2} fluence) showed interesting results. Shown in Fig. 5(a) are R_s vs T plots for irradiated 2400 Å microstrip resonator obtained at 4.88 GHz at 0 and 0.8 T fields; Fig. 5(b) shows R_s vs T plots at 0 and 0.8 T fields for the same sample at 9.55 GHz. The corresponding plots of this resonator at 0.8 T obtained at 4.88 and 9.55 GHz frequencies before irradiation are also shown for comparison

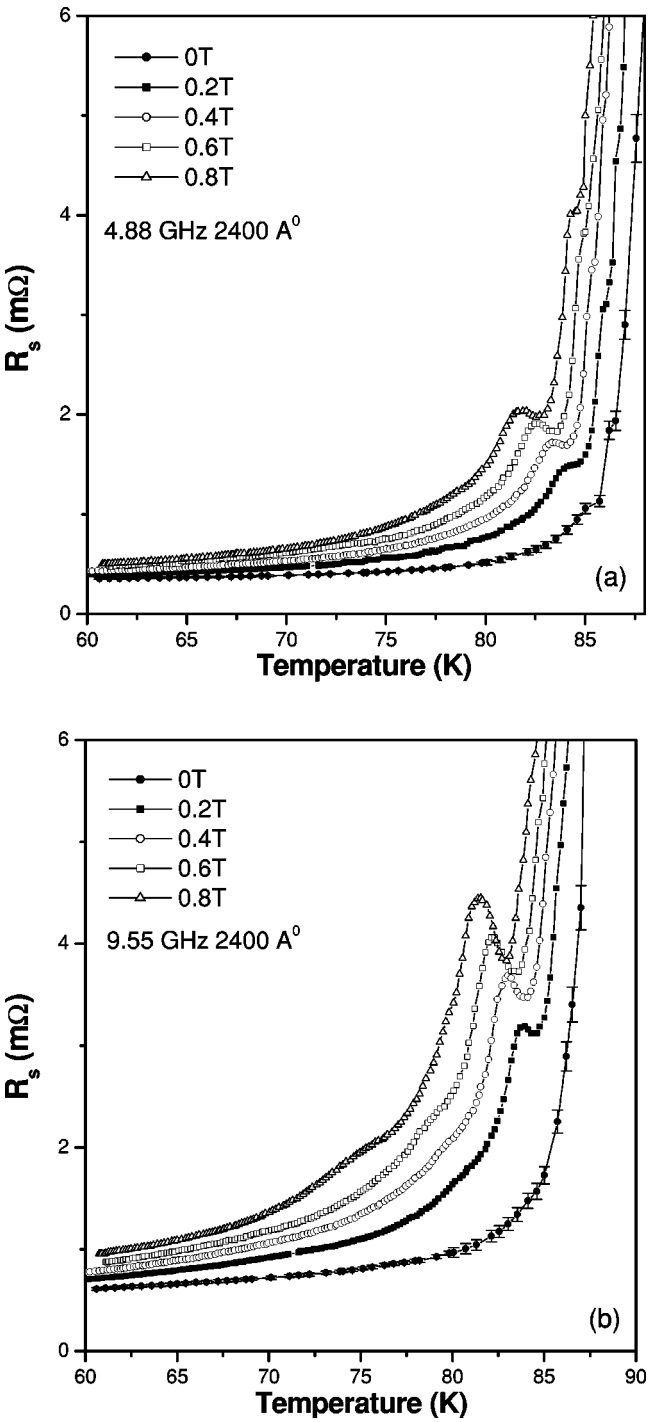

FIG. 1. R_s vs T plots at 10 dB m microwave power obtained at dc fields in the range 0–0.8 T for 2400 Å thick DBCO microstrip resonators: (a) 4.88 GHz, (b) 9.55 GHz.

in Figs. 5(a) and 5(b), respectively. It may be noted that while there is a slight suppression of peak at 4.88 GHz (as compared to that obtained for the pristine sample), there is a sharp enhancement of peak at 9.55 GHz in the irradiated sample. The R_s vs T plots obtained for the irradiated 3800 Å microstrip resonator showed equally interesting results. Shown in Fig. 6(a) are the R_s vs T plots of this sample for 0 and 0.8 T fields obtained at 4.88 GHz. Figure 6(b) shows

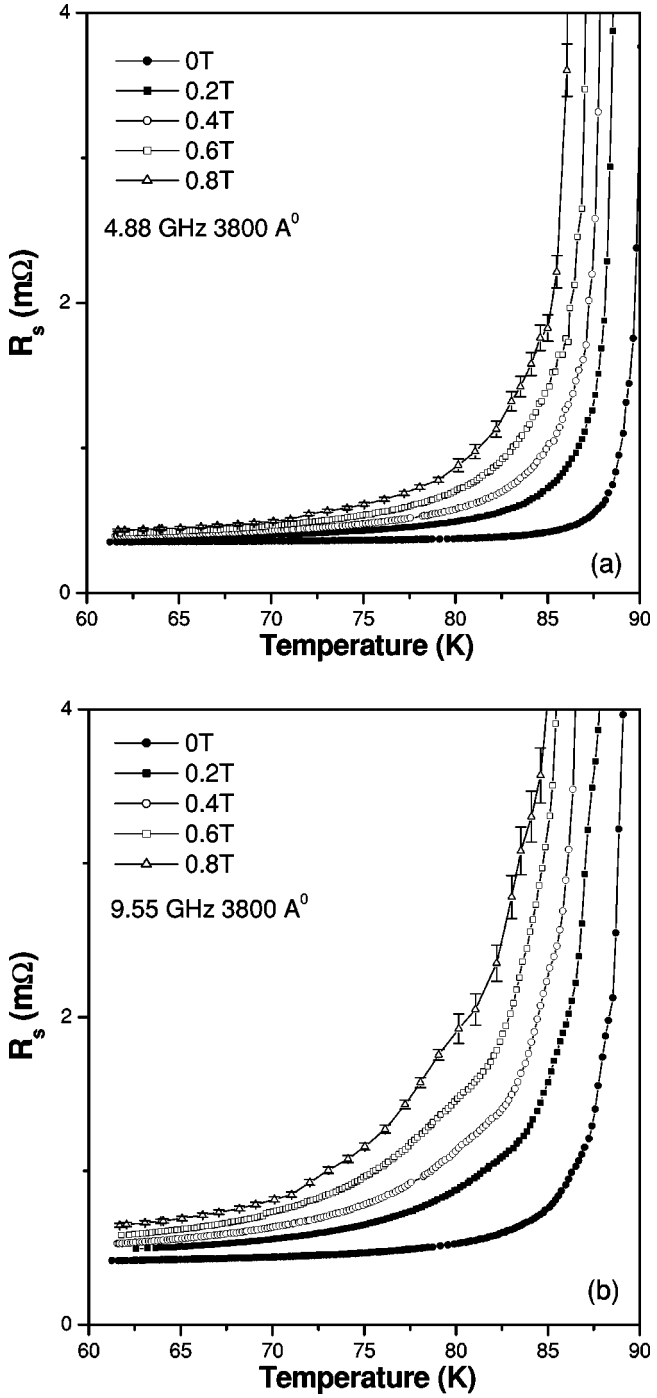

FIG. 2. R_s vs T plots at 10 dB m microwave power at dc fields in the range 0–0.8 T ($H//c$) for 3800 thick DBCO films: (a) 4.88 GHz; (b) 9.55 GHz.

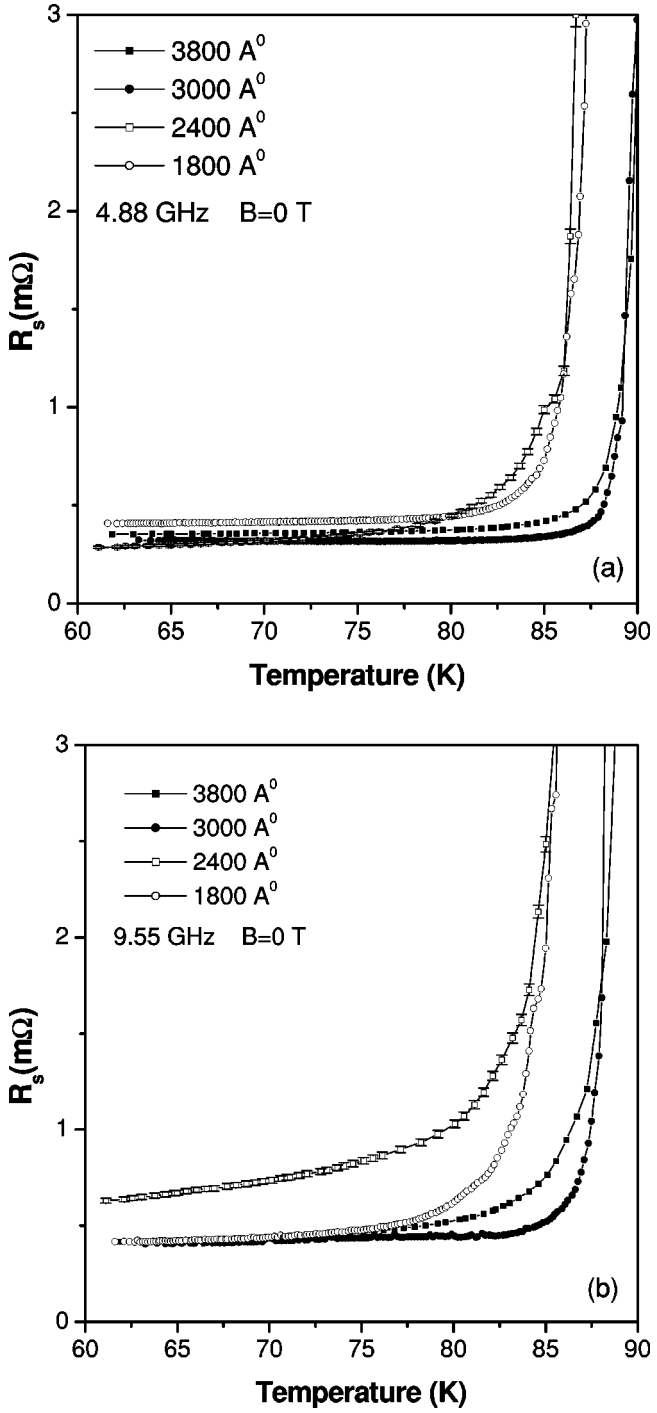

FIG. 3. Zero field R_s vs T plots for various film thickness, at 10 dB m microwave power: (a) at 4.88 GHz, (b) at 9.55 GHz.

similar plots of this sample obtained at 0 and 0.8 T fields at 9.55 GHz. The corresponding plots of this resonator at 0.8 T obtained at 4.88 and 9.55 GHz frequencies before irradiation are also shown for comparison in Figs. 6(a) and 6(b), respectively. In both cases, distinct signatures of peaks are seen at 0.8 T field which were absent in the pristine sample. The 3000 Å film too has shown peak signatures at 0.8 T field at 4.88 and 9.55 GHz frequencies after irradiation.

An important aspect of the microstrip resonator technique is that since R_s increases nearly exponentially as one approaches T_c, Q factor decreases sharply. This obviously means that it is very difficult to measure normal state R_s with this technique as the errors increase as one approaches T_c. Typical errors in R_s measurement are $\pm 5\%$ just below T_c, although they are small ($<2\%$) well below T_c. It is because of these errors near T_c that the experimental plots are not smooth and show minor steplike features near T_c, although they are smooth well below T_c. For the sake of clarity, error

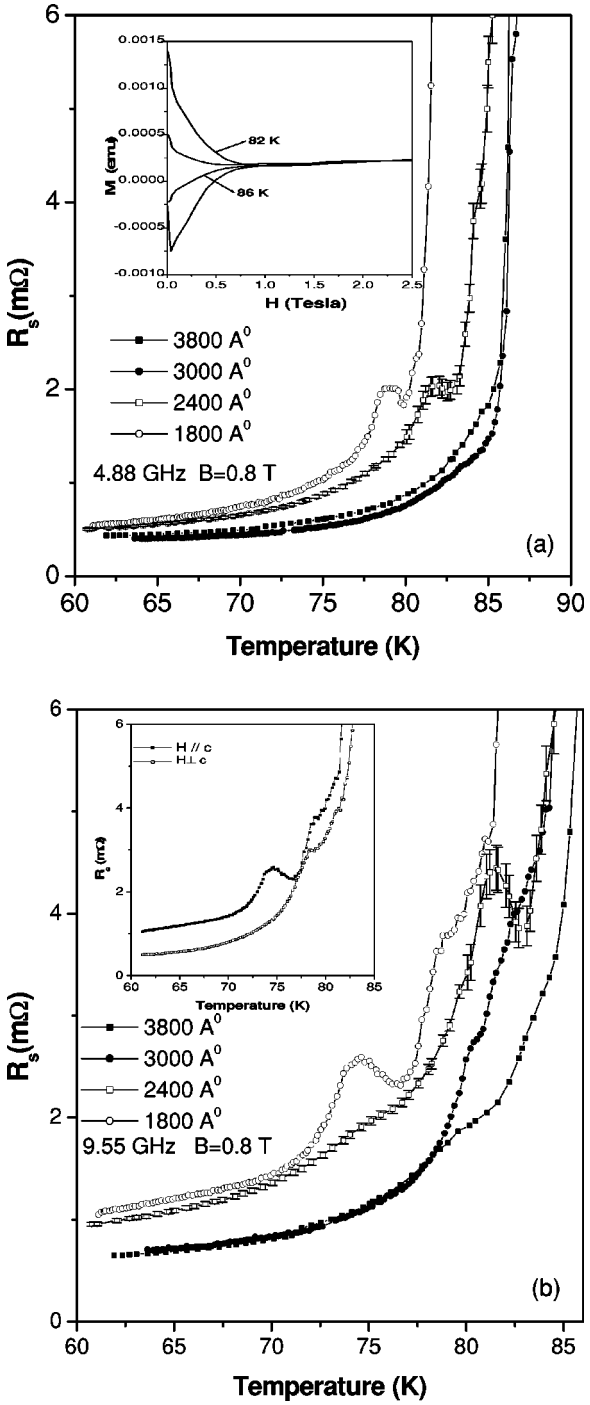

FIG. 4. R_s vs T plots at 0.8 T ($H\|c$) for various film thickness, at 10 dB m microwave power: (a) at 4.88 GHz, inset shows M vs H measurements carried out on an identical DBCO film (2400 Å) at various temperatures; (b) at 9.55 GHz, inset shows R_s vs T plot for 1800 Å film at 0.8 T for $H\|c$ and $H\perp c$ at 9.55 GHz.

bars are shown only on one representative plot in each figure. It may also be mentioned that the repeatability of measurements is very good on a given film (resonator) with variations $\leqslant \pm 2\%$; the nature of the plots, however, varied from film to film depending upon their quality determined primarily by film thickness and LAO substrate.

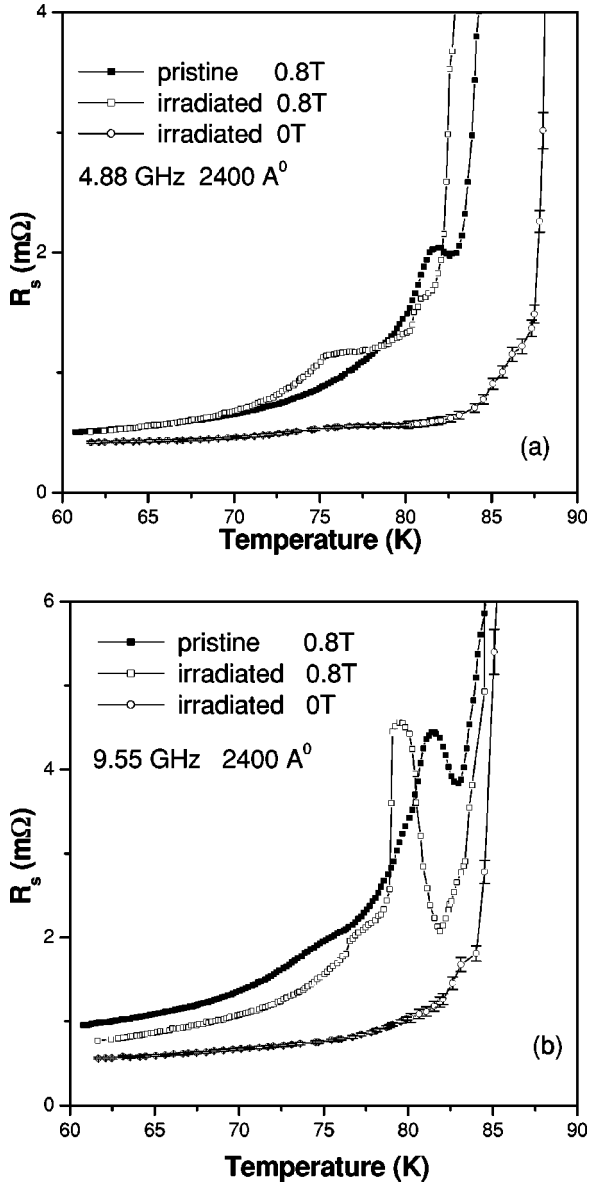

FIG. 5. R_s vs T plots at 10 dB m microwave power at 0 and 0.8 T ($H//c$) fields for 2400 Å thick DBCO film after Ag ion irradiation: (a) 4.88 GHz; (b) 9.55 GHz. Also shown for comparison are the corresponding R_s vs T plots at 0.8 T obtained before irradiation.

IV. DISCUSSION

The high-frequency response of type-II superconductors is characterized by Z_s, the surface impedance, given by $Z_s = R_s + iX_s$. R_s determines dissipation and yields information about the vortex dynamics governed by pinning centers and their energy distribution, whereas X_s, the surface reactance determines Λ, the magnetic-field dependent complex penetration depth. Λ contains λ_v, the vortex penetration depth (complex), λ the London penetration depth, and $\delta_n f$, the quasiparticle skin depth.

A vortex line oscillates under the influence of a rf field and its motion is limited by frictional and pinning forces. Therefore, even in the linear regime the rf field leads to an enhanced dissipation as ω approaches ω_p. The simplest the-

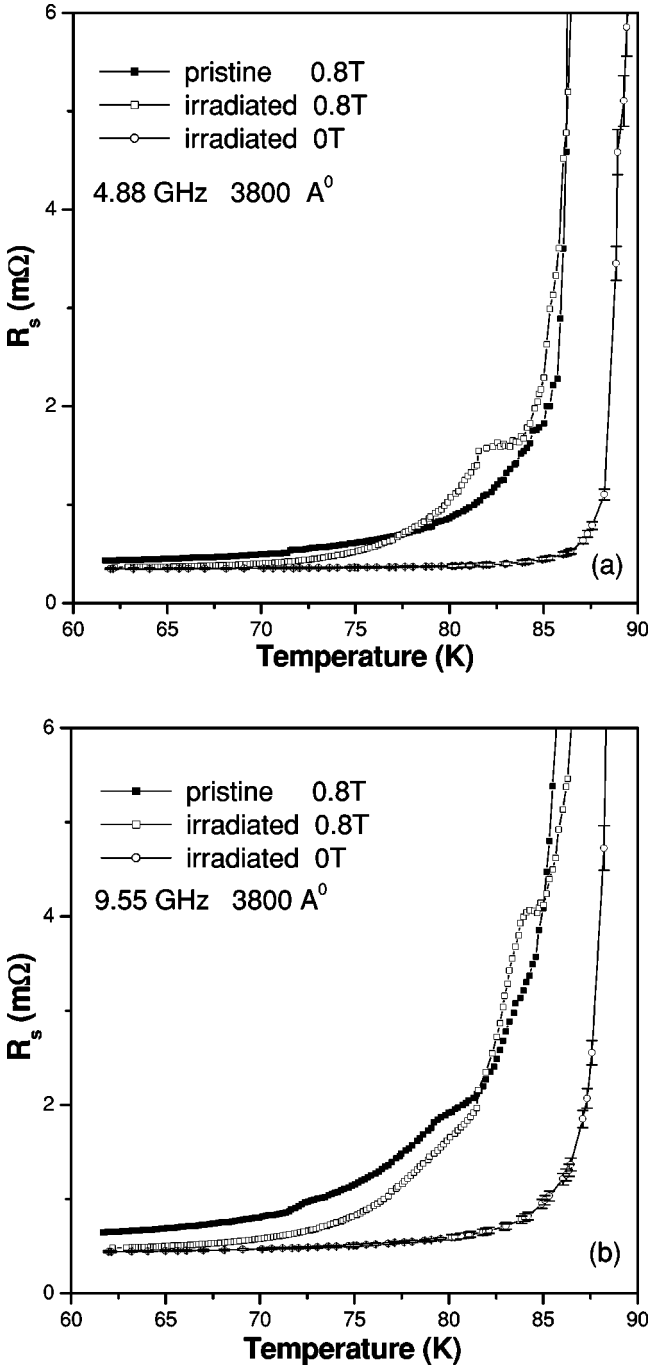

FIG. 6. R_s vs T plots at 10 dB m microwave power at 0 and 0.8 T ($H//c$) fields for 3800 Å thick DBCO film after Ag ion irradiation: (a) 4.88 GHz; (b) 9.55 GHz. Also shown for comparison are the corresponding R_s vs T plots at 0.8 T obtained before irradiation.

oretical model of linear vortex dynamics in rf currents is given by the equation of motion suggested by Gittleman and Rosenblum[18] and thereafter refined by Coffey and Clem.[19] In the microwave regime with frequencies >1 GHz, the vortices are less sensitive to flux creep in YBCO thin films as shown by Revenaz *et al.*,[20] and reiterated by Golosovsky *et al.*[21] Since our measurement frequencies are >1 GHz, we used the Rosenblum and Gittleman equation due to its simplicity. For a massless vortex line oscillating close to the minimum of the pinning potential (in the linear regime at low rf power levels) and experiencing a restoring force κ_p (determined by the curvature of the pinning potential), the equation of motion, neglecting Hall and stochastic thermal force, is given as

$$\eta\dot{x}+\kappa_p x=\frac{J\phi_0}{c}, \tag{1}$$

where $J(T)$ is the microwave driving current, x is the displacement from equilibrium, $\eta=\phi_0 H_{c2}/\rho_n$ is the Bardeen-Stephen viscous drag coefficient, ϕ_0 is the flux quantum, and ρ_n is the normal-state resistivity. Equation (1) leads to the vortex impedance

$$\rho_v=\frac{\phi_0 B}{\eta\left(1+i\frac{\omega_p}{\omega}\right)}=\frac{\omega^2-i\omega\omega_p}{\omega^2+\omega_p^2}\frac{H}{H_{c2}}\rho_n, \tag{2}$$

where H is the applied magnetic field. Equation (2) leads to R_s as a function of ω and ω_p.[7]

$$R_s=\left(\frac{H}{H_{c2}}\rho_n\right)^{1/2}\left[\frac{\mu_0\omega^2}{\sqrt{\omega^2+\omega_p^2}}\left(\frac{\omega_p}{2\sqrt{\omega^2+\omega_p^2}}+1\right)\right]^{1/2}, \tag{3}$$

where $\omega_p=\kappa_p/\eta$ separates the low-frequency regime ($\omega<\omega_p$) dominated by pinning with inductive response, from a high-frequency regime ($\omega>\omega_p$) of free vortex flow with dissipation. In other words, ω_p is the characteristic frequency at which the pinned vortex segments are no longer able to move fast enough to remain in phase with the applied microwave field. From Eq. (3) we see that for $\omega\ll\omega_p$, $R_s=C\sqrt{\omega^2/\omega_p}$, whereas for $\omega\gg\omega_p$, $R_s=D\sqrt{\omega}$, where C and D are constants. It may also be mentioned that although theoretically when $H=0$, Eq. (3) vanishes (that is, the vortex contribution to R_s vanishes), our *zero-field* data imply measurements done at the low remnant field of the magnet (6–10 Oe); hence, $H\neq 0$ but very low in this case.

Material disorder creates pinning centers whose density and energy distribution determine J_c, R_s, λ, and ω_p.[7,22] Unlike high quality weakly pinned DBCO/YBCO crystals, thin films have a high density of point defects such as oxygen vacancies and impurities. Thin films can also have other growth defects such as twin boundaries, stacking faults, etc., which are extended defects. In high quality epitaxial DBCO/YBCO thin films point defects and twin boundaries (propagated through the twinned $LaAlO_3$ substrate) play a vital role in governing the key transport parameters such as J_c, R_s, λ, and ω_p.[23] The high density of point defects is responsible for high J_c in DBCO/YBCO thin films. Point defects also decrease the quasiparticle scattering time $\tau(T)$ and hence, decrease the quasiparticle (normal fluid) contribution to R_s as $R_s\alpha\sigma_1$, where σ_1 is the real part of the conductivity associated with the normal-fluid response:

$$\sigma_1=\left(\frac{1}{\mu_0\lambda^2(0)}\right)X_n(T)\left(\frac{\tau(T)}{1+\omega^2\tau^2(T)}\right), \tag{4}$$

where $X_n(T)$ is the normal-fluid fraction of surface reactance. Therefore, at ''zero'' or very low applied fields, the measured R_s contains primarily the quasiparticle contribution. As the field is increased a larger number of point defects pin the vortices, thus reducing the number available for scattering; this increases the total (measured) R_s and hence, decreases ω_p too as a first approximation (since $R_s \alpha 1/\sqrt{\omega_p}$ for $\omega \ll \omega_p$). In other words, it is logical that since experimental evidence shows that point defects in DBCO/YBCO films lead to low values of R_s then it must be extended defects that are responsible for the observed PE in R_s at microwave frequencies.

It should be mentioned that an important feature of DBCO/YBCO films is that while the point defects are prevalent throughout the thickness of the films, the extended defects such as twins (which are transmitted from the twinned LAO substrates) are primarily confined to the substrate-film interface. This is clear from our earlier work (Srinivasu *et al.*, Ref. 23) which has shown that while J_c increases, R_s decreases with increasing thickness of YBCO films. This implies that the areal density of point defects increases as the thickness increases,[23] while the twin density remains virtually constant. In other words, the ratio $r = n_e/n_p$ of areal density of twins and other LAO-DBCO interface-related extended defects n_e to the areal density of point defects n_p decreases as the film thickness increases. Hence, an evidence for the type of defects responsible for the PE at microwave frequencies could be obtained by a study of the thickness dependence of R_s.

The R_s vs T plots in Figs. 1(a) and 1(b) indicate that for the 2400 Å thick film there is no peak in R_s at zero field, but it evolves gradually with increasing field, that is, gradually with increasing vortex density. On the other hand, for the 3800 Å thick film [Figs. 2(a) and 2(b)], there is no evolution of peak with increasing field, although a slight signature of peak can be seen at the highest field of 0.8 T. All the films of varying thickness do not show PE at zero applied field as seen in Figs. 3(a) and 3(b). On the other hand, the dependence of peak in R_s on film thickness is clearly seen at the applied field of 0.8 T in Fig. 4. Once again, a weak signature of peak in thicker (3000 Å and 3800 Å) films is seen at 0.8 T only at the higher frequency of 9.55 GHz. The peaks in thinner films are also stronger at the higher frequency of 9.55 GHz than at 4.88 GHz.

The plots shown in the above figures were obtained in the linear regime at 10 dB m microwave power. This was confirmed by carrying out R_s measurements at lower power levels of 0, 2, and 5 dB m, all of which neither showed a decrease in R_s nor a shift in the position of peaks both at 4.88 and 9.55 GHz. The linear regime indicates that our measurements are at subcritical (microwave) currents. The dc critical currents measured in these films using microbridges are 2×10^6 A cm^{-2} at 77 K. No peak effect was observed in transport J_c. Further, isothermal magnetization vs field (M-H) measurements performed on thick as well as thin films in the field range 0–2.5 T using a quantum design superconducting quantum interference device (SQUID) magnetometer did not show a peak in the M-H plots. [See inset in Fig. 4(a).]

Two observations are important in the above experimental results. The first is that the conventional PE seen in dc or low-frequency J_c vs $T(H)$ plots is not seen in transport J_c vs T and M-H measurements carried out in the DBCO/YBCO thin films; and the second is that PE at subcritical currents at microwave frequencies is seen only in thinner films and thicker films show only a weak signature of PE. The first observation can be explained by the fact that the high density of defect disorder (point defects as well as extended defects) in thin films suppresses the PE in the J_c vs T or M-H measurements. This is because the J_c vs $T(H)$ plot of a heavily pinned system forms an envelope over the peak region of J_c vs $T(H)$ plot which would have otherwise appeared if the system were weakly pinned. This explanation is supported by the numerous reported results which indicate that the conventional PE is seen only in weakly pinned single crystals ($NbSe_2$, YBCO, etc.).[15] The second observation gives evidence to our earlier conjecture that extended defects such as twins in the films may be responsible for microwave PE. The fact that the ratio n_e/n_p decreases with increasing film thickness can be related to the decreasing signature of microwave PE. Another feature of twins is that they have an angular dependence. The inset in Fig. 4(b) shows a comparison of R_s vs T plots of 1800 Å thick films at $H = 0.8$ T obtained with $H \| c$ and $H \perp c$. A distinct angular dependence of PE is seen which can only be explained as due to extended defects such as twins and not due to random pinning disorder caused by point defects. Higher R_s in the $H \| c$ plot is also in agreement with the reported results of Anand and Tinkham[24] who have observed higher dissipation with $H \| c$ than $H \perp c$ in YBCO thin films.

In order to further understand the role of extended defects on PE at microwave frequencies, we investigated the effect of columnar defects (which are extended defects) generated by 200 MeV Ag ions. The three microstrip resonators with thicknesses 2400 Å, 3000 Å, and 3800 Å whose pristine plots are shown Figs. 1–4 were chosen for irradiation. The plots in Figs. 5 and 6 show very interesting results. The plots shown in Figs. 5(a) and 5(b) were obtained for the 2400 Å film after 200 MeV Ag irradiation at 4×10^{10} ions cm^{-2} (matching field of 0.8 T) at 4.88 GHz and 9.55 GHz, respectively. We notice that the 81 K peak at 4.88 GHz is somewhat suppressed after irradiation and there is another weak peak at the lower temperature of 75 K. The behavior at 9.55 GHz, however, is different; here, the 81 K peak becomes prominent and the new peak at 75 K is insignificant. The plots of 3800 thick sample [Figs. 6(a) and 6(b)] are equally interesting. This sample had shown an insignificant PE signature in the pristine state (Fig. 2); after the generation of columnar defects, however, distinct peaks are seen at 0.8 T both at 4.88 GHz and 9.55 GHz. It is also interesting to note that, as observed earlier,[7] the dissipation (R_s) at any given temperature, except the peak region, is generally lower in the irradiated films at the matching field of 0.8 T.

While the above experiments show a clear pointer to the extended defects such as substrate twins and columnar defects being responsible for PE at microwave frequencies, it is possible to ask if this PE could be due to finite-size effects. Finite-size effects can arise due to the fact that thicknesses of

these films are comparable to penetration depth of films. Our earlier work (Ref. 17) indicates that the London penetration depth of similar (YBCO) films at 77 K, λ (77 K) $\sim$2500 Å with $\lambda(0)\sim$1450 Å. Since only thinner films (thickness $\leqslant$2400 Å) show microwave PE in the temperature range 75–80 K, it is possible to argue that this finite-size effect could be the cause of microwave PE. In order to investigate this possibility and also to find out if the substrate-related twins are indeed responsible for microwave PE, we carried out another experiment with the aim of growing twin-free DBCO film. Obviously we had to use twin-free LAO substrates. Although LAO is a very good microwave compatible substrate, it is very difficult to obtain untwinned LAO substrates. Nevertheless, a comparison of the above results with the results obtained with a low-twinned LAO substrate was made. Figure 7(a) shows this comparison at 0.8 T and 4.88 GHz. Clearly, the 2400 Å DBCO film on the low-twinned substrate does not show any PE signature. However, as the measurement frequency is increased to 9.55 GHz, peak appears at 0.8 T even in this low-twinned DBCO film as shown in Fig. 7(b). The inset in Fig. 7(a) shows an optical micrograph of normal LAO substrate obtained with differential interference contrast (DIC). The inset in Fig. 7(b) shows a similar optical micrograph of a low-twinned LAO substrate. A much higher density of twins can be clearly seen in the normal LAO as compared to the low-twinned LAO. It may also be noted that the low-twinned substrates which give films with low twin density cause low dissipation (low R_s) at any given temperature as seen in Figs. 7(a) and 7(b). Hence, the above observations, viz., the appearance of microwave PE in 3800 Å DBCO film after generation of CD's with Ag ion irradiation as well as the absence of microwave PE at 4.88 GHz in 2400 Å DBCO film grown on low-twinned LAO substrate suggest that the observed microwave PE is not due to finite-size effects.

The conventional PE in J_c vs T (or H) observed in twinned YBCO and in some low-temperature superconductor crystals has been related to the twin structure.[15,25] In twin-free crystals, the PE has been related to intrinsic pinning from CuO planes or second-phase impurities. In twinned YBCO crystals the peak has been found to depend strongly on the orientation of the applied field relative to the twin planes. Peak has been found to be largest for vortex motion along the twin planes and applied field parallel to c axis and weakest if the field is tilted out of the plane of the twins. In pure YBCO crystals, oxygen vacancy clusters—but not point defects due to individual oxygen vacancies—have also been related to PE in J_c.[22] Further, depending upon their nature, radiation induced defects have also been found to affect the peak, although the radiation induced point defects have not been related to change in J_c or the peak. In other words, the conventional PE is crucially dependent on the defect structure and is not intrinsic to the crystal structure.

Our experimental observations too led us to the conclusion that the PE observed by us in R_s vs T plots at subcritical currents at microwave frequencies also is not intrinsic to the crystal structure of the DBCO film but to the nature of the defects in the film. Evidence indicates that the extended defects such as twins at the substrate-film interface propagated from the LAO substrate or columnar defects created due to Ag ion irradiation, but not the point defects, are responsible for this PE at microwave frequencies. However, the similarity between the conventional PE in J_c and the microwave PE in R_s ends here.

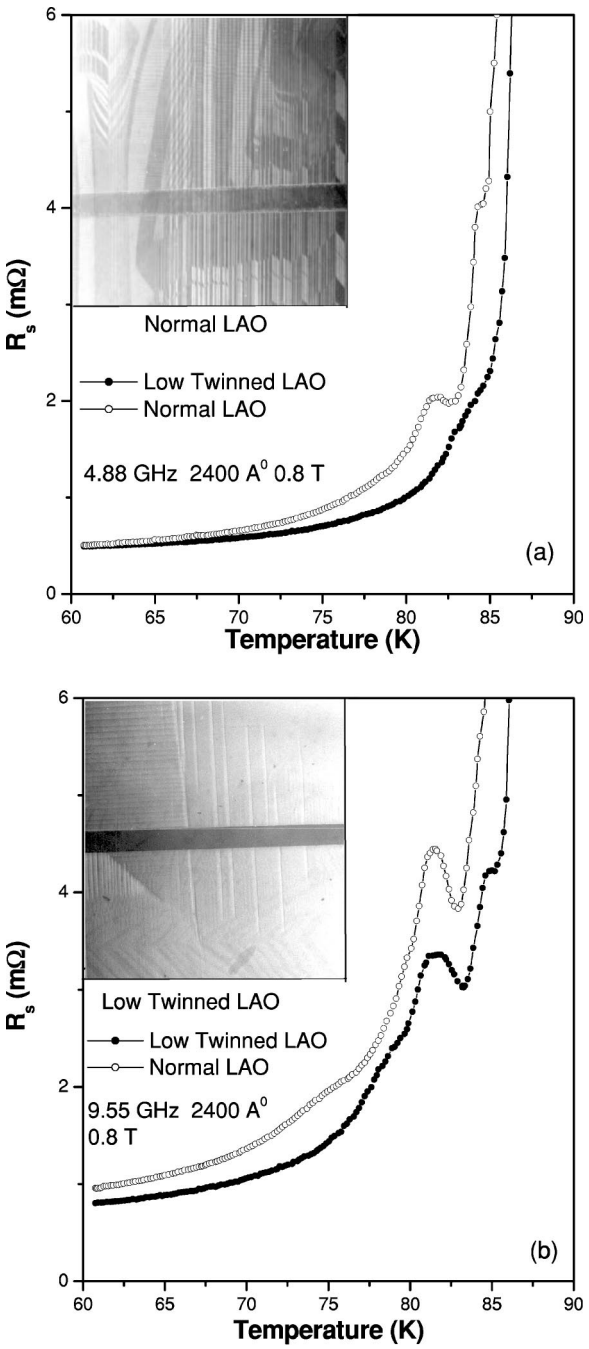

FIG. 7. Comparison of R_s vs T plots at 10 dB m microwave power at 0.8 T obtained for 2400 Å thick DBCO films grown on normal and low-twinned LAO substrates: (a) 4.88 GHz [inset—optical micrograph of resonator on normal LAO obtained with DIC); (b) 9.55 GHz (inset—optical micrograph of resonator on low-twinned LAO obtained with DIC).

While the conventional PE in J_c vs $T(H)$ plots is observed in a driven vortex lattice,[6] the central parameter which controls vortex dynamics at subcritical currents at mi-

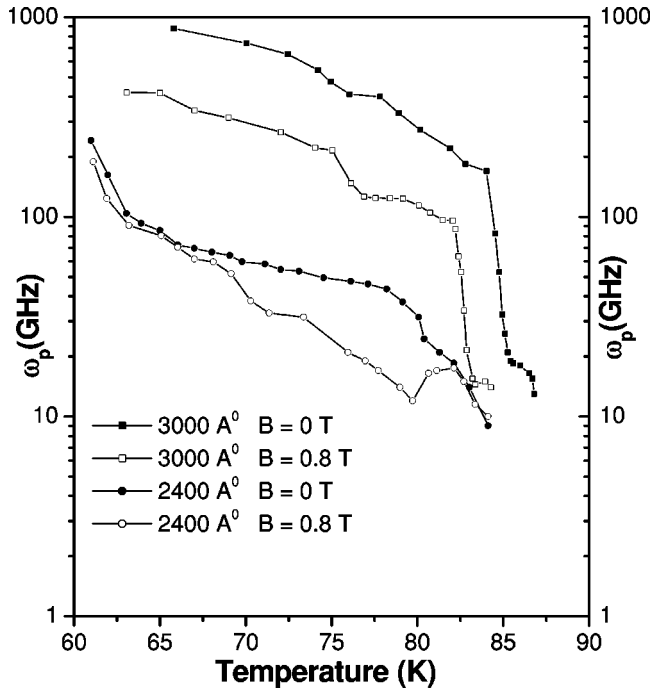

FIG. 8. Variation of ω_p with temperature for 2400 Å and 3000 Å films at 0 and 0.8 T.

crowave frequencies is not J_c but $\omega_p = \kappa_p / \eta$, which in turn is dependent on the nature and distribution of pinning centers. ω_p also depends upon the viscosity coefficient $\eta = \phi_0 H_{c2} / \rho_n$. Since PLD grown DBCO thin films have a distribution of defects—both correlated extended defects and uncorrelated point defects—the characteristic depinning frequency ω_p of the film can be considered (as a first-order approximation) as an effective sum of depinning frequencies $\omega_{p1}, \omega_{p2}, \ldots$ associated with different sets of defects, each of which would be determined by their density, pinning constant κ_p, and viscosity coefficient η. Since the areal density of point defects is lower in thinner films as compared to thicker ones, ω_p of these films is mainly determined by the characteristic ω_{p1} associated with the interfacial defects such as twin boundaries. As the film thickness increases, the relative areal density of point defects increases, and although ω_p is governed both by ω_{p1} (of the extended defects) and ω_{p2} of the point defects, it is increasingly dominated by ω_{p2}. Hence, thicker films with a higher areal density of point defects as compared to the interfacial extended defects show low R_s, high ω_p, and no PE as observed by us.

While showing experimental evidence and arguing that extended defects such as twins and CD's are responsible for microwave PE in R_s vs $T(H)$ plots at subcritical microwave currents, we have not shown if κ_p and η (or both these parameters of the extended defects) are responsible for the observed PE. This obviously requires further extensive investigations. However, we have calculated the values of ω_p from Eq. (3) both for thinner and thicker films using the values of R_s at 4.88 and 9.55 GHz. Shown in Fig. 8 are the ω_p vs T plots obtained for 2400 Å and 3000 Å thick films at 0 and 0.8 T. As expected, the 3000 Å film shows high ω_p values both for 0 T and 0.8 T. On the other hand, the thinner (2400 Å) film shows smaller ω_p values. Equally important is the peak seen in ω_p vs T plot of 2400 Å film at 0.8 T, which is a result of the peaks in R_s vs T plots of this film at the measurement frequencies 4.88 GHz and 9.55 GHz.

A quantitative explanation for the conventional PE phenomenon occurring in J_c in a driven vortex lattice was given by Pippard[26] many years ago who proposed that the increase in J_c is associated with the softening of the shear modulus C_{66}. Subsequently, Larkin and Ovchinnikov[16] presented a more quantitative explanation of this PE as arising from the softening of all the elastic moduli of the vortex lattice near H_{c2}. The main similarity between the conventional PE in J_c and microwave PE in R_s is that both are governed by a particular type of defects which act as characteristic pinning centers. Further, in both cases, the peak shifts to lower temperatures as the applied field is increased. Therefore, we can attribute microwave PE phenomenon to a softening of the (weakly pinned) ordered vortex lattice and a consequent transformation into a more strongly pinned amorphous solid or a pinned liquid phase.[3] Alternatively, one can also think of a plastic flow of vortex array involving the formation of channels in which the vortex array is more ordered and weakly pinned than in the surrounding areas resulting in a rise in R_s. Subsequent jamming or blocking of these channels by strong pins (extended defects) hinders the flow of vortex arrays, thus reducing R_s. Possibility of weakly pinned channels has been proposed in low-frequency ac current.[27,28] However, the precise mechanism responsible for microwave PE in R_s is difficult to be explained at this stage with the existing experimental observations. What we can say at present is that a particular set of extended defects which have characteristic ω_p values are responsible for the observed microwave PE in R_s. Further, our observations of the dependence of microwave PE on the measurement frequency indicates that a dominant set of extended defects having characteristic ω_p values (determined by pinning constant and viscosity η) govern the position and the intensity of the peaks in the R_s vs T plots.

V. CONCLUSION

In conclusion, we have investigated the dynamics of vortices at subcritical currents at microwave frequencies in epitaxial DBCO thin films in the thickness range 1800 Å–3800 Å. Experimental evidence shows that a higher areal density of point defects in thicker films cause a low value of R_s and high ω_p as compared to thinner films. Occurrence of a peak in R_s in dc magnetic fields in films of varying thickness is governed by the nature and concentration of defects. We have shown that extended defects such as twin boundaries are primarily responsible for peak in R_s with dc magnetic fields; whereas the large areal density of point defect disorder in thicker films causes low R_s, high ω_p, and does not give rise to a peak. These results are also supported by measurements carried out on DBCO films grown on low-twinned LAO substrates which did not show PE at the lower frequency 4.88 GHz, but only at higher frequency 9.55 GHz. Independent evidence for extended defects being responsible for microwave PE has also been obtained via generation of

columnar defects using Ag ion irradiation. Even thicker films which did not show PE in the pristine state showed PE after the introduction of columnar defects by irradiation. While these experimental results lead us to believe that extended defects are responsible for the observed PE at microwave frequencies, further investigations are needed to find out the role of κ_p and η associated with the extended defects in causing microwave PE. The ω_p values calculated from experimental R_s vs T data at 4.88 and 9.55 GHz frequencies show that ω_p decreases with increasing temperature and field, as expected. Further, while thicker films show high values of ω_p at all temperatures, the thinner film (2400 Å) which has a peak in the R_s vs T plots also shows a peak in the ω_p vs T plot.

ACKNOWLEDGMENTS

The authors wish to thank A. K. Nigam for SQUID measurements and S. Bhattacharya for helpful discussions. We would like to thank G. V. Ravindra and R. D. Bapat for discussions.

[1] G. Blatter, M.V. Feigel'man, V.B. Geshkenbein, A.I. Larkin, and V.M. Vinokur, Rev. Mod. Phys. **66**, 1125 (1994).
[2] W. Henderson, E.Y. Andrei, M.J. Higgins, and S. Bhattacharya, Phys. Rev. Lett. **80**, 381 (1998); M. Golosovsky, M. Tsindlekht, and D. Davidov, Supercond. Sci. Technol. **9**, 1 (1996).
[3] A.R. Bhangale, P. Raychaudhuri, S. Sarkar, T. Banerjee, S.S. Bhagwat, V.S. Shirodkar, and R. Pinto, Phys. Rev. B **63**, 180502(R) (2001).
[4] A. Pautrat, C. Goupil, C. Simon, N. Lutke-Entrup, B. Placais, P. Mathieu, Y. Simon, A. Rykov, and S. Tajima, Phys. Rev. B **63**, 054503 (2001).
[5] H. Kupfer, A.A. Zhukov, A. Will, W. Jan, R. Meier-Hirmer, Th. Wolf, V.I. Voronkova, M. Klaser, and K. Saito, Phys. Rev. B **54**, 644 (1996); Th. Wolf, A-C. Bornarel, H. Kupfer, R. Meier-Hirmer, and B. Obst, *ibid.* **56**, 6308 (1997).
[6] W.K. Kwok, J.A. Fendrich, C.J. vander Beek, and G.W. Crabtree, Phys. Rev. Lett. **73**, 2614 (1994).
[7] T. Banerjee, D. Kanjilal, and R. Pinto, Phys. Rev. B **65**, 174521 (2002).
[8] J. Owliaei, S. Sridhar, and J. Taivacchio, Phys. Rev. Lett. **69**, 3366 (1992).
[9] M.S. Pambianchi, D.H. Wu, L. Ganapathi, and A. Anlage, IEEE Trans. Appl. Supercond. **3**, 2774 (1993).
[10] S. de Brion, R. Calemczuk, and J.Y. Henry, Physica C **178**, 225 (1991).
[11] P.L. Gammel, L.F. Schneemeyer, J.V. Waszczak, and D.J. Bishop, Phys. Rev. Lett. **61**, 1666 (1988).
[12] M.J. Higgins and S. Bhattacharya, Physica C **257**, 232 (1996).
[13] S.S. Banerjee, N.G. Patil, S. Saha, S. Ramakrishnan, A.K. Grover, S. Bhattacharya, G. Ravikumar, P.K. Mishra, T.V. Chandrasekhar Rao, V.C. Sahni, M.J. Higgins, E. Yamamoto, Y. Haga, M. Hedo, Y. Inada, and Y. Onuki, Phys. Rev. B **58**, 995 (1998).
[14] J. Shi, X.S. Ling, R. Liang, D.A. Bonn, and W.N. Hardy, Phys. Rev. B **60**, 12 593 (1999).
[15] A.I. Larkin, M.C. Marchetti, and V.M. Vinokur, Phys. Rev. Lett. **75**, 2992 (1995); C. Tang, X.S. Ling, S. Bhattacharya, and P.M. Chaikin, Europhys. Lett. **35**, 597 (1996).
[16] A.I. Larkin and Y.N. Ovchinnikov, J. Low Temp. Phys. **34**, 409 (1979).
[17] R. Pinto, N. Goyal, S.P. Pai, P.R. Apte, L.C. Gupta, and R. Vijayaraghavan, J. Appl. Phys. **73**, 5105 (1993); R. Pinto, D. Kaur, M.S.R. Rao, P.R. Apte, V.V. Srinivasu, and R. Vijayaraghavan, Appl. Phys. Lett. **68**, 1720 (1996).
[18] J.I. Gittleman and B. Rosenblum, Phys. Rev. Lett. **16**, 734 (1996).
[19] M. Coffey and J. Clem, Phys. Rev. Lett. **67**, 386 (1991); Phys. Rev. B **46**, 11 757 (1992).
[20] S. Revenaz, D.E. Oates, D. Labbe-Lavigne, G. Dresselhaus, and M.S. Dresselhaus, Phys. Rev. B **50**, 1178 (1994).
[21] M. Golosovsky, M. Tsindlekht, H. Chayet, and D. Davidov, Phys. Rev. B **50**, 470 (1994).
[22] H. Kupfer, Th. Wolf, C. Lessing, A.A. Zhukov, X. Lancon, R. Meier-Hirmer, W. Schauer, and H. Wuhl, Phys. Rev. B **58**, 2886 (1998).
[23] W.N. Hardy, S. Kamal, D.A. Bonn, K. Zhang, R. Liang, E. Klein, D.C. Morgan, and D.J. Barr, Physica B **197**, 609 (1994); V.V. Srinivasu, J. Jesudasan, D. Kaur, R. Pinto, and R. Vijayaraghavan, Appl. Supercond. **6**, 45 (1998).
[24] N. Anand and M. Tinkham, Phys. Rev. B **52**, 3784 (1995).
[25] A.A. Zhukov, H. Kupfer, H. Claus, and H. Wuhl, Phys. Rev. B **52**, R9871 (1995).
[26] A.P. Pippard, Philos. Mag. **19**, 217 (1969).
[27] W. Henderson and E.Y. Andrei, Phys. Rev. Lett. **81**, 2352 (1998).
[28] M.-C. Cha and H.A. Fertig, Phys. Rev. Lett. **80**, 3851 (1998).